

# New iridium complexes(III) bearing 2-phenylimidazo[4,5-f][1,10]-phenanthroline ligand: Synthesis, characterization, electrochemical and photoluminescence studies

Cigdem Sahin\*, Murat Sahin

Department of Chemistry, Art&Science Faculty, Pamukkale University, Denizli, Turkey



## ARTICLE INFO

### Article history:

Received 8 June 2020  
Revised 5 October 2020  
Accepted 6 October 2020  
Available online 7 October 2020

### Keywords:

Iridium complex  
Counterion  
Photoluminescence  
Phenanthroline

## ABSTRACT

Iridium complexes bearing 2-phenylimidazo[4,5-f]-[1,10]-phenanthroline with different substituents (-CH<sub>3</sub>, -CH(CH<sub>3</sub>)<sub>2</sub>, -OCH<sub>3</sub>, -C<sub>6</sub>H<sub>5</sub>) were synthesized and characterized. The effects of different substituents and solvents on the photoluminescence properties of the complexes with [Cl] and [PF<sub>6</sub>] counter anions have been investigated. The synthesized complexes show high photoluminescence quantum yield due to the extension of the  $\pi$ -electron conjugation of 2-phenylimidazo[4,5-f][1,10]-phenanthroline ligands. The results indicate that the choice of counter anions ([Cl] and [PF<sub>6</sub>]) has an important influence on the quantum yield of the complexes. In toluene, the compound 4 with phenyl substituent exhibits excimer emission with increasing solution concentrations in the presence of [Cl] counter anion. The linear correlation was observed between the redox potentials of the complexes and Hammett Substituent Constants. The linear correlation can allow the prediction of the effects of substituents on electrochemical studies.

© 2020 Elsevier B.V. All rights reserved.

## 1. Introduction

In recent years, phosphorescent metal complexes such as ruthenium, iridium or platinum have attracted interest due to their potential applications in optoelectronic devices [1], chemoreceptors [2], biosensors [3]. Among these complexes, iridium complexes are the most popular in organic light emitting diodes (OLEDs) due to color tunability, shorter radiative lifetime and high quantum yields [4,5]. The high quantum yields of iridium complexes are related to mixing the singlet and the triplet excited states by strong spin-orbit coupling [6,7]. The photochemical, photophysical and electrochemical properties of iridium complexes can be tuned by varying the ligands [6]. The design of ancillary ligands can affect the quantum yield, excited state dynamics, HOMO and LUMO energy levels which are important to improve the efficiency of OLED devices [8,9]. 2-phenylimidazo[4,5-f][1,10]-phenanthroline derivatives as ancillary ligands can be good candidates for the iridium complexes due to rigid structure and their extended conjugation [10]. The rigid conjugated ligands in iridium complexes can lead to efficient spin-orbit coupling which can decrease nonradiative transitions. This may result an increase in the quantum yields of iridium complexes [11,12]. The counterions of the complexes can also have an important effect on photophysical properties. The choice

of counter anions can influence intermolecular interaction, molecular aggregation and concentration quenching process for the complexes [13,14].

In this work, iridium complexes bearing 2-phenylimidazo[4,5-f]-[1,10]-phenanthroline with different substituents (-CH<sub>3</sub>, -CH(CH<sub>3</sub>)<sub>2</sub>, -OCH<sub>3</sub>, -C<sub>6</sub>H<sub>5</sub>) and 2-(3-fluorophenyl)-4-methylpyridine were synthesized. Our aim in synthesis of the complexes is to increase the quantum yield of the molecules by using conjugated ligands. The complexes exhibit high quantum yield in the presence of 2-phenylimidazo[4,5-f][1,10]-phenanthroline derivatives as ancillary ligands. The effect of [Cl] and [PF<sub>6</sub>] counter anions on electrochemical and photophysical properties of the complexes have been investigated. The thermal, electrochemical and photophysical properties of the synthesized complexes can be appropriate for OLED applications.

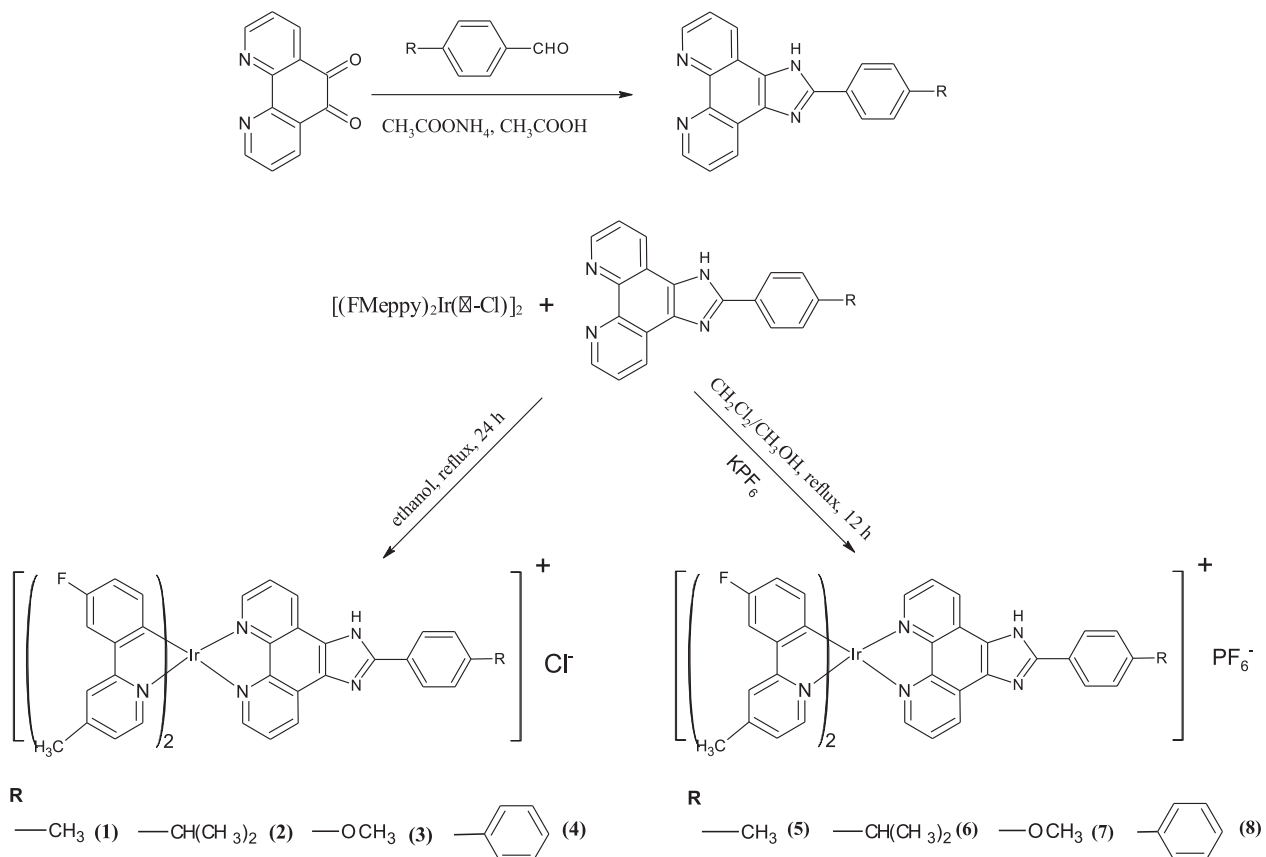
## 2. Experimental section

### 2.1. Materials

Iridium(III) trichloride hydrate, 3-fluoro phenylboronic acid, 2-bromo-4-methylpyridine, 1,10-phenanthroline, tetrabutylammonium hexafluorophosphate (TBAPF<sub>6</sub>), tetrakis(triphenylphosphine) palladium(0) were provided from Aldrich. 4-methoxybenzaldehyde and potassium hexafluorophosphate was obtained from Alfa Aesar. 4-isopropylbenzaldehyde, 4-biphenylcarboxaldehyde, p-

\* Corresponding author.

E-mail address: [cigdemsahin82@gmail.com](mailto:cigdemsahin82@gmail.com) (C. Sahin).

**Scheme 1.** Synthetic route of the compounds (1–8).

tolualdehyde were obtained from Acros. 1,10-phenanthroline-5,6-dione [15], 2-(3-fluorophenyl)-4-methylpyridine (FMeppy) [16] and [(FMeppy)<sub>2</sub>Ir(μ-Cl)]<sub>2</sub> [17] were prepared according to the literature. All reactions were performed using standard Schlenk techniques under argon atmosphere.

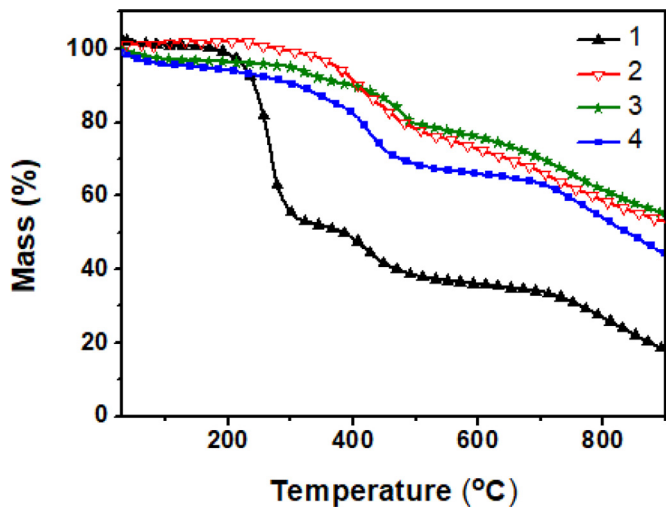
## 2.2. Measurements

The absorption and photoluminescence (PL) measurements were performed using Shimadzu UV-1601 UV-Vis spectrophotometer and Perkin Elmer LS55 fluorescence spectrometer, respectively. Mass spectra were obtained using Bruker Microflex LT MALDI-TOF MS. ATR-FTIR spectra were performed using Perkin Elmer Spectrum Two FT-IR Spectrometer with a diamond ATR. NMR spectra were obtained using Varian VNMRJ 400 NMR instrument. Tetramethylsilane (TMS) was used as reference material for the reported chemical shifts. The thermal data of the complexes were obtained by Netzsch STA 449F5 instrument. Electrochemical data were recorded on CH Instrument 660 B Model Electrochemical Workstation.

## 2.3. Synthesis and characterization

### 2.3.1. Synthesis of ligands

2-(4-methylphenyl)-1H-imidazo-[4,5-f]-[1,10]-phenanthroline (L<sub>1</sub>) [18], 2-(4-isopropyl phenyl)-1H-imidazo-[4,5-f]-[1,10]-phenanthroline (L<sub>2</sub>), 2-(4-methoxyphenyl)-1H-imidazo-[4,5-f]-[1,10]-phenanthroline (L<sub>3</sub>) [19,20], 2-([1,1'-biphenyl]-4-yl)-1H-imidazo-[4,5-f]-[1,10]-phenanthroline (L<sub>4</sub>) [21] were prepared according to the literature procedures starting from p-tolualdehyde, isopropylbenzaldehyde, 4-methoxybenzaldehyde, 4-biphenylcarboxaldehyde, respectively. A mixture of aldehyde (0.12

**Fig. 1.** TGA curves of the compounds (1–4).

mmol), 1,10-phenanthroline-5,6-dione (0.12 mmol), ammonium acetate (2.38 mmol) and glacial acetic acid (4.5 mL) was refluxed for 5 h under argon atmosphere. After the mixture was cooled to room temperature, the solution was neutralized with aqueous ammonia solution. The resulting solid was filtered and washed with ethanol. The dried product was obtained as a yellow powder.

2-(4-methylphenyl)-1H-imidazo-[4,5-f]-[1,10]-phenanthroline (L<sub>1</sub>): 57% yield. FTIR (ATR, cm<sup>-1</sup>): 3346, 3021-3041, 2881-2921, 1606, 1551. <sup>1</sup>H NMR (CDCl<sub>3</sub>, 400 MHz) δ ppm: 8.82 (s, 4H), 8.14 (d, 2H), 7.42 (s, 2H), 7.20 (d, 2H), 2.30 (s, 3H). <sup>13</sup>C NMR (DMSO-d<sub>6</sub>,

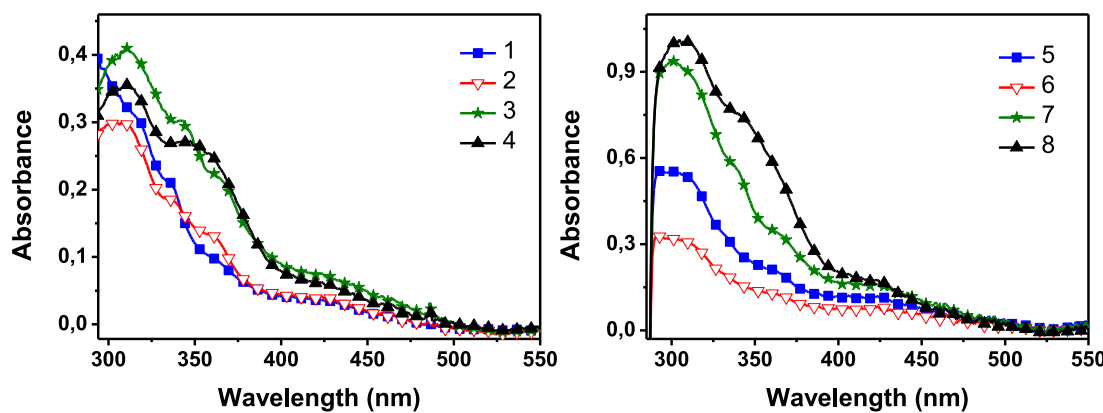


Fig. 2. UV-Vis absorption spectra of  $3 \times 10^{-6}$  M solution of the compounds (1–8) in chlorobenzene.

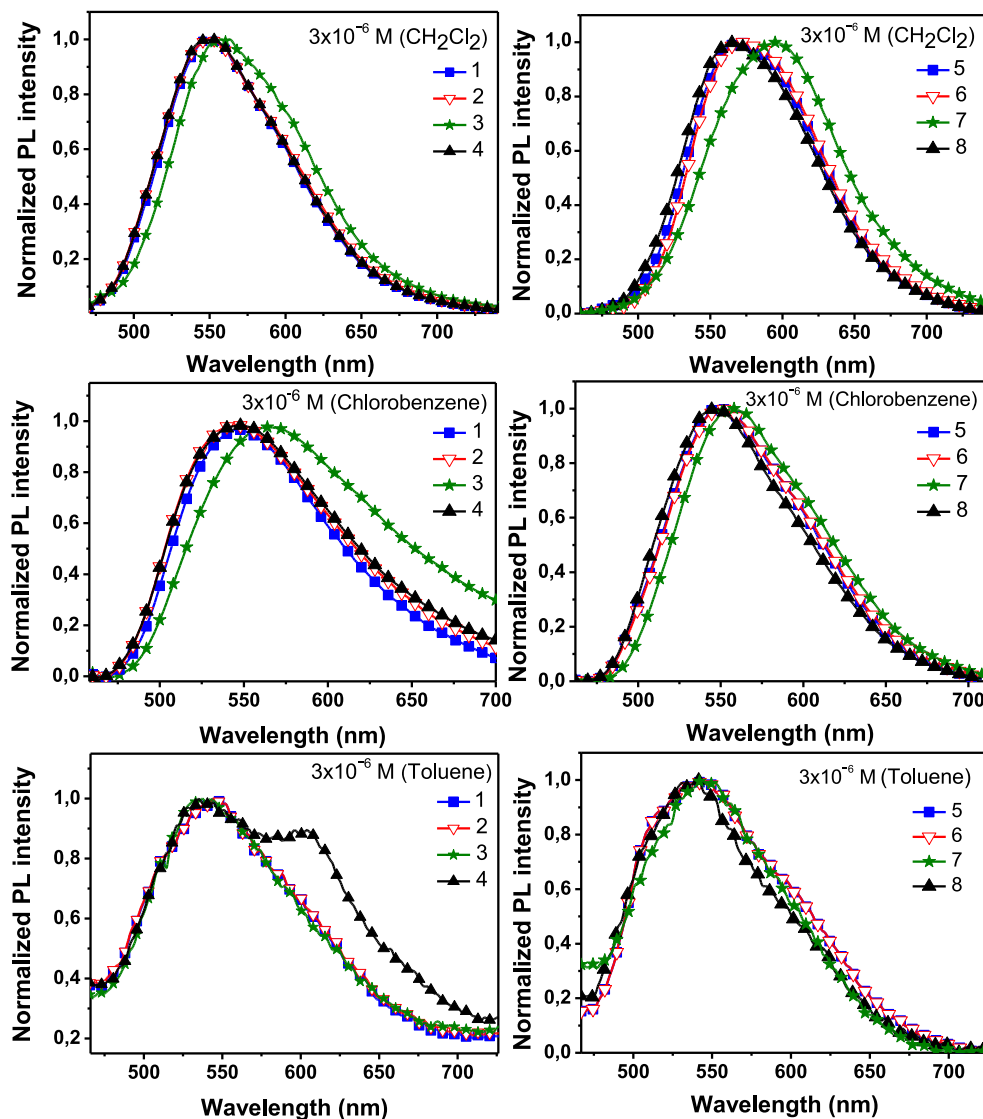
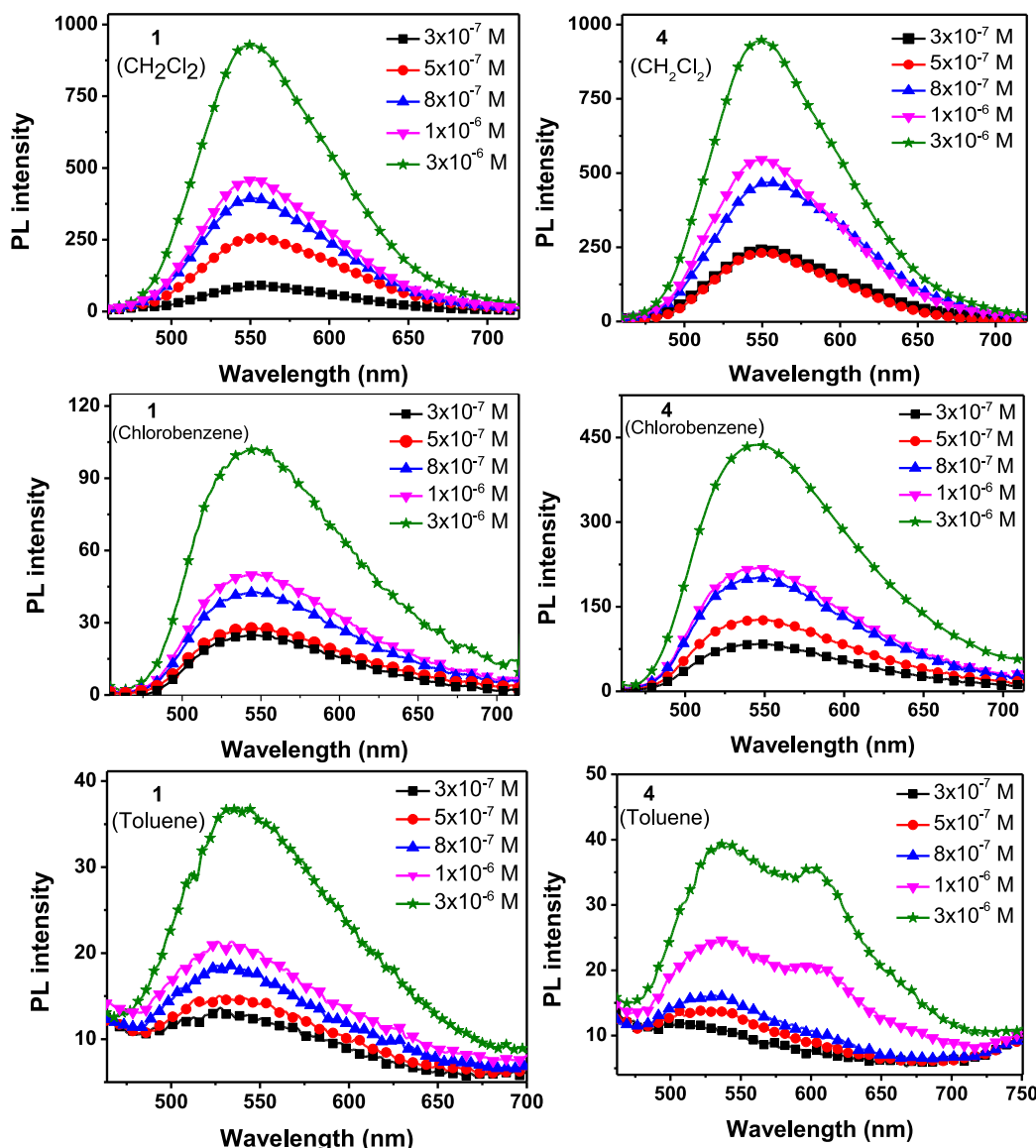
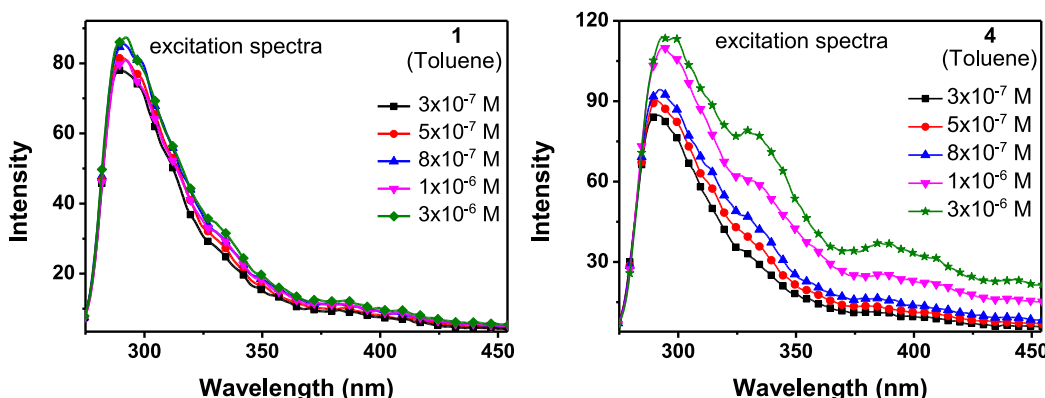


Fig. 3. PL spectra of  $3 \times 10^{-6}$  M solution of the compounds (1–8) in different solvents ( $\text{CH}_2\text{Cl}_2$ , chlorobenzene, toluene).



**Fig. 4.** PL spectra of  $3 \times 10^{-7}$  M,  $5 \times 10^{-7}$  M,  $8 \times 10^{-7}$  M,  $1 \times 10^{-6}$  M,  $3 \times 10^{-6}$  M solutions of the compounds (1 and 4) in different solvents (dichloromethane, chlorobenzene, toluene).



**Fig. 5.** The excitation spectra of  $3 \times 10^{-7}$  M,  $5 \times 10^{-7}$  M,  $8 \times 10^{-7}$  M,  $1 \times 10^{-6}$  M,  $3 \times 10^{-6}$  M solutions of the compounds (1 and 4) in toluene.

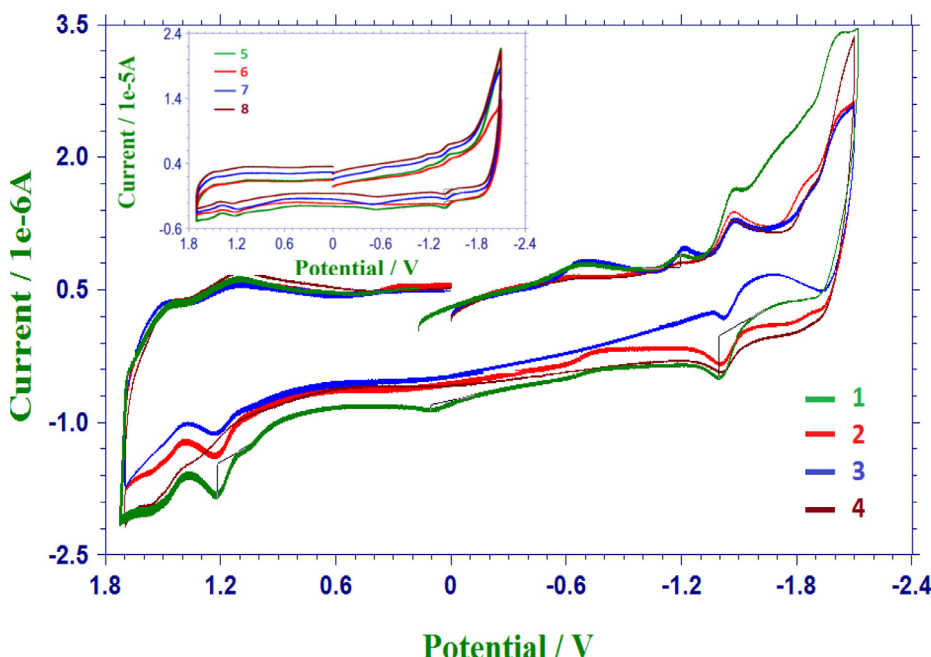


**Fig. 6.** Cyclic voltammograms of the compounds (1–8) measured with scan rate is  $100\text{ mV s}^{-1}$  in acetonitrile solution.

100.57 MHz)  $\delta$  ppm: 151.3, 148.2, 143.8, 139.9, 130.0, 127.6, 126.7, 123.8, 21.4. MALDI-TOF MS (m/z): 311.430 [M+H]<sup>+</sup>.

2-(4-isopropylphenyl)-1H-imidazo-[4,5-f]-[1,10]-phenanthroline ( $L_2$ ): 64% yield. FTIR (ATR,  $\text{cm}^{-1}$ ): 3380, 3030–3060, 2930–2965, 1605, 1543.  $^1\text{H}$  NMR ( $\text{CDCl}_3$ , 400 MHz)  $\delta$  ppm: 9.03 (d, 2H), 8.95 (d, 2H), 8.24 (d, 2H), 7.21 (d, 2H), 7.03 (d, 1H), 6.95 (d, 1H), 2.51 (d, 1H), 1.65 (d, 6H).  $^{13}\text{C}$  NMR ( $\text{DMSO}-d_6$ , 100.57 MHz)  $\delta$  ppm: 152.1, 148.3, 142.9, 139.5, 131.1, 127.3, 126.4, 123.5, 30.2, 22.8. MALDI-TOF MS (m/z): 339.372 [M+H]<sup>+</sup>.

2-(4-methoxyphenyl)-1H-imidazo-[4,5-f]-[1,10]-phenanthroline ( $L_3$ ): 52% yield. FTIR (ATR,  $\text{cm}^{-1}$ ): 3375, 3040–3065, 2890–2910, 1603, 1576.  $^1\text{H}$  NMR ( $\text{CDCl}_3$ , 400 MHz)  $\delta$  ppm: 9.9 (d, 1H), 9.01 (d, 1H), 8.17 (s, 1H), 8.04 (s, 1H), 7.85 (d, 2H), 7.52 (d, 1H), 7.02 (d, 3H), 6.95 (s, 1H), 3.90 (t, 3H).  $^{13}\text{C}$  NMR ( $\text{DMSO}-d_6$ , 100.57 MHz)  $\delta$  ppm: 160.9, 151.3, 148.2, 143.7, 131.7, 130.1, 128.9, 123.9, 114.9, 55.8. MALDI-TOF MS (m/z): 327.189 [M+H]<sup>+</sup>.

2-([1,1'-biphenyl]-4-yl)-1H-imidazo-[4,5-f]-[1,10]-phenanthroline ( $L_4$ ): 60% yield. FTIR (ATR,  $\text{cm}^{-1}$ ): 3372, 3050–3080, 1605, 1548.  $^1\text{H}$  NMR ( $\text{CDCl}_3$ , 400 MHz)  $\delta$  ppm: 8.82 (s, 2H), 8.76 (d, 2H) 8.26 (d, 2H) 7.55 (t, 3H), 7.35 (m, 6H).  $^{13}\text{C}$  NMR ( $\text{DMSO}-d_6$ , 100.57 MHz)  $\delta$  ppm: 150.9, 148.3, 146.3, 143.87, 139.63, 130.6, 130.2, 129.6, 129.5, 129.4, 127.3, 127.1, 123.8. MALDI-TOF MS (m/z): 373.504 [M+H]<sup>+</sup>.

### 2.3.2. Synthesis of iridium complexes (1–4)

The corresponding compounds (1–4) were prepared using a modified literature procedure [22]. [(FMeppy)<sub>2</sub>Ir( $\mu$ -Cl)]<sub>2</sub> (0.022 mmol) and phenanthroline ligand (0.047 mmol) were refluxed in ethanol (7 mL) for 24 h under argon atmosphere. After the mixture was cooled to room temperature, the product precipitated with diethyl ether. The solid was collected by filtration and precipitated again from dichloromethane/diethyl ether for purification. The product was obtained as yellow solid.

Starting from  $L_1$ ,  $L_2$ ,  $L_3$ ,  $L_4$  ligands, [Ir(FMeppy)<sub>2</sub> $L_1$ ][Cl], [Ir(FMeppy)<sub>2</sub> $L_2$ ][Cl], [Ir(FMeppy)<sub>2</sub> $L_3$ ][Cl], [Ir(FMeppy)<sub>2</sub> $L_4$ ][Cl] were prepared, respectively (Scheme 1).

[Ir(FMeppy)<sub>2</sub> $L_1$ ][Cl] (1): 58% yield. FTIR (ATR,  $\text{cm}^{-1}$ ): 3403, 3037, 2958, 2921, 1621, 1548, 1480, 1456, 1380, 1267, 1121, 820, 739.  $^1\text{H}$  NMR ( $\text{CDCl}_3$ , 400 MHz)  $\delta$  ppm: 10.56 (s, 1H), 9.32 (d,

1H), 8.63 (d, 2H) 8.21 (d, 1H), 8.10 (d, 1H), 7.76 (d, 2H), 7.67 (d, 1H), 7.61 (d, 1H), 7.43 (dt, 1H) 7.35 (d, 2H), 7.15 (d, 1H), 7.11 (d, 1H), 7.07 (d, 1H), 6.77 (td, 2H), 6.67 (dd, 2H), 6.56 (d, 1H), 6.28 (dt, 2H), 2.48 (d, 3H), 2.42 (d, 6H).  $^{13}\text{C}$  NMR ( $\text{DMSO}-d_6$ , 100.57 MHz)  $\delta$  ppm: 167.47, 165.62, 158.92, 151.09, 148.86, 146.01, 144.50, 140.85, 132.42, 132.09, 132.05, 130.24, 129.06, 127.65, 127.04, 125.70, 124.65, 121.66, 117.56, 117.37, 111.88, 101.67, 21.46, 21.01. MALDI-TOF MS (m/z): 874.872 [M-Cl]<sup>+</sup>.

[Ir(FMeppy)<sub>2</sub> $L_2$ ][Cl] (2): 56% yield. FTIR (ATR,  $\text{cm}^{-1}$ ): 3375, 3046, 2960, 2923, 1621, 1548, 1479, 1442, 1362, 1263, 1176, 811, 748.  $^1\text{H}$  NMR ( $\text{CDCl}_3$ , 400 MHz)  $\delta$  ppm: 10.56 (s, 1H), 9.28 (s, 1H), 8.64 (d, 2H), 8.23 (d, 1H), 8.13 (m, 1H), 7.76 (m, 2H), 7.67 (d, 1H), 7.61 (d, 1H), 7.43 (dd, 3H), 7.16 (d, 1H), 7.11 (d, 1H), 7.07 (d, 1H), 6.77 (td, 2H), 6.66 (m, 2H), 6.55 (s, 1H), 6.29 (d, 2H), 2.97 (m, 1H), 2.48 (d, 3H), 2.42 (d, 3H), 1.29 (d, 6H).  $^{13}\text{C}$  NMR ( $\text{DMSO}-d_6$ , 100.57 MHz)  $\delta$  ppm: 167.23, 166.23, 165.62, 158.96, 153.48, 151.07, 148.67, 145.54, 144.50, 144.24, 142.36, 140.88, 132.00, 130.22, 129.00, 127.02, 125.69, 124.64, 121.64, 117.56, 112.00, 103.07, 33.2, 22.10. MALDI-TOF MS (m/z): 904.838 [M+1-Cl]<sup>+</sup>.

[Ir(FMeppy)<sub>2</sub> $L_3$ ][Cl] (3): 69% yield. FTIR (ATR,  $\text{cm}^{-1}$ ): 3389, 3045, 2948, 2910, 1615, 1547, 1479, 1440, 1362, 1249, 1177, 819, 743.  $^1\text{H}$  NMR ( $\text{CDCl}_3$ , 400 MHz)  $\delta$  ppm: 10.52 (s, 1H), 9.30 (d, 2H), 8.69 (m, 2H), 8.09 (m, 2H), 7.77 (d, 2H), 7.68 (d, 1H), 7.61 (d, 1H), 7.44 (m, 2H), 7.16 (d, 1H), 7.07 (m, 2H), 6.77 (m, 2H), 6.69 (d, 1H), 6.65 (d, 1H), 6.59 (m, 1H), 6.31 (t, 1H), 6.25 (m, 1H), 3.87 (dd, 3H), 2.50 (dd, 3H), 2.43 (dd, 3H).  $^{13}\text{C}$  NMR ( $\text{DMSO}-d_6$ , 100.57 MHz)  $\delta$  ppm: 167.67, 166.25, 165.63, 161.56, 161.47, 161.28, 158.91, 151.31, 151.09, 148.86, 145.56, 144.25, 139.52, 132.69, 132.43, 129.70, 128.75, 127.49, 127.31, 125.70, 125.24, 124.64, 123.91, 121.67, 117.37, 115.07, 110.00, 104.83, 55.89, 21.02. MALDI-TOF MS (m/z): 890.958 [M-Cl]<sup>+</sup>.

[Ir(FMeppy)<sub>2</sub> $L_4$ ][Cl] (4): 69% yield. FTIR (ATR,  $\text{cm}^{-1}$ ): 3368, 3034, 2963, 2908, 1619, 1546, 1476, 1441, 1362, 1260, 1176, 806, 794.  $^1\text{H}$  NMR ( $\text{CDCl}_3$ , 400 MHz)  $\delta$  ppm: 10.58 (s, 1H), 9.25 (s, 1H), 8.79 (d, 2H), 8.22 (d, 1H), 8.11 (d, 1H), 7.73 (dd, 4H), 7.65 (m, 4H), 7.46 (t, 3H), 7.38 (d, 1H), 7.21 (s, 1H), 7.11 (d, 2H), 6.78 (td, 2H), 6.72 (m, 1H), 6.66 (t, 1H), 6.58 (m, 1H), 6.32 (t, 1H), 6.25 (m, 1H), 2.48 (s, 3H), 2.43 (s, 3H).  $^{13}\text{C}$  NMR ( $\text{DMSO}-d_6$ , 100.57 MHz)  $\delta$  ppm: 165.63, 162.57, 161.27, 158.96, 152.39, 151.09, 148.89, 145.63,

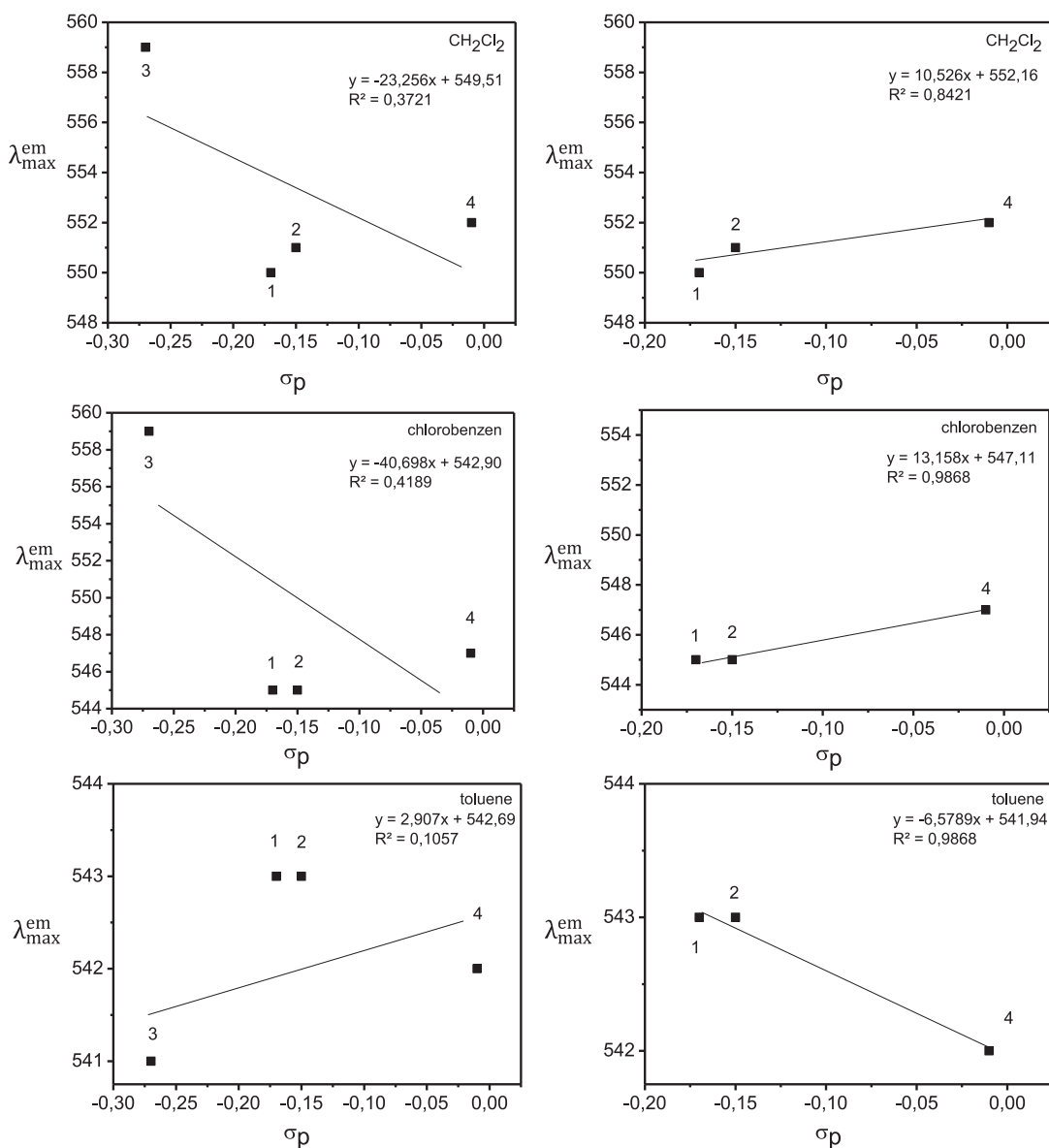


Fig. 7. The correlation between  $\sigma_p$  and emission maxima of the compounds (1–4).

144.61, 144.46, 144.22, 142.33, 141.15, 139.49, 132.49, 129.56, 129.12, 128.70, 128.56, 128.26, 127.84, 127.65, 127.47, 127.17, 125.66, 124.65, 123.82, 119.00, 105.23, 103.03, 21.02. MALDI-TOF MS (m/z): 937.863 [M-Cl]<sup>+</sup>.

### 2.3.3. Synthesis of iridium complexes (5-8)

The corresponding compounds (5-8) were prepared using procedure described in the literature with slight modifications [23].  $[(\text{FMeppy})_2\text{Ir}(\mu\text{-Cl})_2$  (0.022 mmol) and corresponding phenanthroline ligand (0.047 mmol) were refluxed in dichloromethane/methanol (6 mL, 2:1, v/v) for 12 h under argon atmosphere. After the mixture was cooled to room temperature,  $\text{KPF}_6$  (12 mmol) was added and stirred for 3 hours. The obtained solid was collected by filtration and precipitated again from dichloromethane/diethyl ether for purification. The product was obtained as yellow solid.

Starting from  $\text{L}_1$ ,  $\text{L}_2$ ,  $\text{L}_3$ ,  $\text{L}_4$  ligands,  $[\text{Ir}(\text{FMeppy})_2\text{L}_1][\text{PF}_6]$ ,  $[\text{Ir}(\text{FMeppy})_2\text{L}_2][\text{PF}_6]$ ,  $[\text{Ir}(\text{FMeppy})_2\text{L}_3][\text{PF}_6]$ ,  $[\text{Ir}(\text{FMeppy})_2\text{L}_4][\text{PF}_6]$  were prepared, respectively (Scheme 1).

$[\text{Ir}(\text{FMeppy})_2\text{L}_1][\text{PF}_6]$  (5): 61% yield. FTIR (ATR,  $\text{cm}^{-1}$ ): 3368, 3050, 2948, 2888, 1621, 1550, 1483, 1438, 1360, 1276, 1176, 812, 553.  $^1\text{H}$  NMR ( $\text{CDCl}_3$ , 400 MHz)  $\delta$  ppm: 9.93 (s, 1H), 9.23 (d, 1H), 8.42 (d, 2H) 8.17 (dd, 1H), 8.10 (dd, 1H), 7.77 (d, 2H), 7.67 (d, 1H), 7.61 (d, 1H), 7.44 (dd, 1H) 7.34 (d, 2H), 7.18 (d, 1H), 7.13 (d, 1H), 7.09 (d, 1H), 6.77 (td, 2H), 6.67 (dd, 2H), 6.62 (d, 1H), 6.30 (m, 2H), 2.48 (d, 3H), 2.41 (d, 6H).  $^{13}\text{C}$  NMR ( $\text{DMSO}-d_6$ , 100.57 MHz)  $\delta$  ppm: 175.62, 167.45, 166.21, 165.64, 158.91, 153.47, 151.07, 148.85, 145.54, 144.22, 140.86, 132.72, 132.04, 130.22, 129.05, 127.03, 125.67, 124.63, 121.64, 120.92 117.20, 111.84, 105.06, 102.83, 21.44, 20.87.  $^{19}\text{F}$  NMR ( $\text{CDCl}_3$ )  $\delta$  ppm: -71.84 (d, 6F,  $\text{PF}_6$ ), -121.15 (dq, 2F). MALDI-TOF MS (m/z): 874.947 [M- $\text{PF}_6$ ]<sup>+</sup>.

$[\text{Ir}(\text{FMeppy})_2\text{L}_2][\text{PF}_6]$  (6): 59% yield. FTIR (ATR,  $\text{cm}^{-1}$ ): 3358, 3063, 2977, 2951, 1624, 1548, 1478, 1439, 1362, 1275, 1179, 817, 554.  $^1\text{H}$  NMR ( $\text{CDCl}_3$ , 400 MHz)  $\delta$  ppm: 9.90 (s, 1H), 9.26 (s, 1H), 8.43 (d, 2H), 8.17 (d, 1H), 8.10 (d, 1H), 7.77 (m, 2H), 7.67 (d, 1H), 7.61 (d, 1H), 7.43 (td, 3H), 7.17 (d, 1H), 7.10 (d, 1H), 7.06 (d, 1H), 6.78 (td, 2H), 6.68 (m, 3H), 6.29 (m, 2H), 2.99 (m, 1H), 2.49 (d, 3H), 2.43 (d, 3H), 1.30 (d, 6H).  $^{13}\text{C}$  NMR ( $\text{DMSO}-d_6$ , 100.57 MHz)  $\delta$  ppm: 175.64, 167.47, 166.23, 165.62, 155.27, 151.07,

148.86, 146.22, 145.54, 144.50, 142.36, 140.88, 132.72, 132.00, 130.21, 129.01, 127.03, 125.67, 124.65, 121.85, 121.64, 117.56, 112.00, 109.35, 103.07, 33.6, 23.7.  $^{19}\text{F}$  NMR ( $\text{CDCl}_3$ )  $\delta$  ppm: -71.83 (d, 6F,  $\text{PF}_6^-$ ), -121.12 (dq, 2F). MALDI-TOF MS (m/z): 904.527 [ $\text{M}+\text{PF}_6^-$ ]<sup>+</sup>.

[Ir(FMeppy)<sub>2</sub>L<sub>3</sub>][PF<sub>6</sub>] (7): 63% yield. FTIR (ATR,  $\text{cm}^{-1}$ ): 3372, 3066, 2950, 2895, 1615, 1551, 1480, 1439, 1363, 1256, 1179, 812, 555.  $^1\text{H}$  NMR ( $\text{CDCl}_3$ , 400 MHz)  $\delta$  ppm: 9.77 (s, 1H), 9.27 (d, 1H), 8.44 (m, 2H), 8.14 (m, 2H), 7.76 (m, 2H), 7.67 (d, 1H), 7.61 (d, 1H), 7.44 (m, 3H), 7.11 (d, 1H), 7.06 (dd, 2H), 6.78 (td, 2H), 6.70 (m, 2H), 6.62 (d, 1H), 6.29 (m, 2H), 3.88 (d, 3H), 2.49 (d, 3H), 2.43 (d, 3H).  $^{13}\text{C}$  NMR ( $\text{DMSO}-d_6$ , 100.57 MHz)  $\delta$  ppm: 179.70, 168.49, 165.62, 163.40, 161.53, 161.11, 158.91, 151.08, 149.01, 148.74, 148.20, 145.56, 144.38, 142.99, 132.98, 132.48, 132.28, 128.75, 127.59, 127.31, 125.70, 124.63, 122.24, 121.86, 121.11, 117.56, 117.36, 115.07, 111.81, 109.90, 55.80, 20.90.  $^{19}\text{F}$  NMR ( $\text{CDCl}_3$ )  $\delta$  ppm: -71.80 (d, 6F,  $\text{PF}_6^-$ ), -121.44 (dq, 2F). MALDI-TOF MS (m/z): 890.563 [ $\text{M}-\text{PF}_6^-$ ]<sup>+</sup>.

[Ir(FMeppy)<sub>2</sub>L<sub>4</sub>][PF<sub>6</sub>] (8): 67% yield. FTIR (ATR,  $\text{cm}^{-1}$ ): 3363, 3058, 2965, 2907, 1622, 1548, 1477, 1443, 1361, 1265, 1176, 815, 554.  $^1\text{H}$  NMR ( $\text{CDCl}_3$ , 400 MHz)  $\delta$  ppm: 9.44 (s, 2H), 8.43 (m, 2H), 8.23 (dd, 1H), 8.13 (dd, 1H), 7.73 (m, 4H), 7.60 (dd, 4H), 7.45 (td, 3H), 7.39 (d, 1H), 7.21 (d, 1H), 7.12 (m, 2H), 6.79 (td, 2H), 6.73 (m, 1H), 6.66 (t, 1H), 6.59 (td, 1H), 6.32 (dd, 1H), 6.26 (dd, 1H), 2.49 (d, 3H), 2.43 (d, 3H).  $^{13}\text{C}$  NMR ( $\text{DMSO}-d_6$ , 100.57 MHz)  $\delta$  ppm: 179.30, 166.25, 165.63, 159.08, 151.09, 148.89, 145.63, 144.61, 144.45, 144.20, 142.31, 141.22, 139.49, 132.42, 129.56, 129.11, 128.69, 128.55, 127.83, 127.66, 127.45, 127.17, 125.68, 124.65, 121.67, 117.59, 105.19, 102.91, 20.90.  $^{19}\text{F}$  NMR ( $\text{CDCl}_3$ )  $\delta$  ppm: -71.89 (d, 6F,  $\text{PF}_6^-$ ), -121.60 (dq, 2F). MALDI-TOF MS (m/z): 937.458 [ $\text{M}-\text{PF}_6^-$ ]<sup>+</sup>.

### 3. Results and discussion

#### 3.1. Structural characterization

The  $^1\text{H}$  NMR spectrum of L<sub>1</sub> ligand shows proton signal as singlets at 2.29 ppm which is attributed to the -CH<sub>3</sub> substituent on the phenyl ring. The signals at 2.51 ppm and 1.65 ppm are assigned to -CH and methyl groups in L<sub>2</sub> ligand, respectively. Characteristic proton signal of methoxy substituent of L<sub>3</sub> is observed at 3.76 ppm. In addition, the NH proton of imidazole ring is not observed in the  $^1\text{H}$  NMR spectra of phenanthroline ligands. It can be attributed to fast exchange of a proton between the two N atoms of the imidazole ring in solution [20]. The iridium complexes were characterized by  $^1\text{H}$  NMR,  $^{13}\text{C}$  NMR and mass spectroscopies. In the  $^1\text{H}$  NMR spectra of the compounds (1-3 and 5-7), the integrated intensities of aromatic signals exhibit 22 protons (27 protons for compounds 4 and 8) in the range of 9.30-6.30 ppm which can prove the presence of two 2-phenylpyridine and one phenanthroline ligand (Figure S1). In the aliphatic region, the two peaks at 2.48 and 2.42 ppm are associated with the -CH<sub>3</sub> substituent of the 2-phenylpyridine of iridium compounds. The peaks at 7.76 ppm and 6.30 ppm may be associated with the coordination of the NC-type of 2-phenylpyridine as bidentate [24]. The peaks of proton adjacent to N atoms of phenanthroline ligand are shifted from 8.82 ppm to 8.64 ppm upon coordination to iridium. The peak at around 10.56 ppm was observed due to the NH proton of imidazole ring in complexes. It was reported that the NN-type phenanthroline ligands as bidentate can coordinate to iridium in [Ir(C<sup>N</sup>N)<sub>2</sub>(N<sup>N</sup>N)] type complex [11,25]. The proton signals of 1H-imidazo-[4,5-f]-[1,10]-phenanthroline ligands of complexes at 7.61, 7.43, 7.11, 7.07 ppm are good agreement with the reported the related classes of iridium complexes containing 2-phenylpyridine and phenanthroline ligands as bidentate [11,25]. In the  $^{13}\text{C}$  NMR spectra of the compounds, the peaks at around 145.9 ppm and 150.9 ppm are attributed to the cyclometalation carbon of 2-phenylpyridine

bound to iridium atom [26] and the carbon atom adjacent to N atom of 2-phenylpyridine [24], respectively. The carbon signal of phenanthroline ligand at 151 ppm is shifted to 166 ppm with the coordination of ligand to iridium (Figure S2). The  $^{19}\text{F}$  NMR spectra of the compounds (5-8) were obtained to confirm the presence of [PF<sub>6</sub><sup>-</sup>] counterion. The doublet peaks at -71.83 ppm were observed in the presence of [PF<sub>6</sub><sup>-</sup>] anion for compounds (5-8) [27]. The FTIR spectra of molecules show the characteristic peaks for the imidazole N-H stretch around 3375  $\text{cm}^{-1}$ . The mass spectra of the complexes show the parent molecular ion [M-Cl]<sup>+</sup> for complexes 1-4 and [M-PF<sub>6</sub><sup>-</sup>]<sup>+</sup> for complexes 5-8 (Figure S1).

Thermal behaviors of the compounds (1-4) were investigated using thermal gravimetric analysis (TGA) at a heating rate of 10°C/min under nitrogen atmosphere. The mass loss of the iridium compounds is given in Table S1. The synthesized complexes (1-3) show high thermal stability. The decomposition temperatures are 318°C, 346°C and 312°C for complexes 1, 2 and 3, respectively. The high thermal stability can be attributed to the 2-phenylpyridine ligands containing polar F atoms which can induce intermolecular interaction [28].

The TGA curve of compound 1 (Fig. 1) shows two decomposition steps in the temperature range 30-900°C. The first decomposition step of compound 1 occurs between 30°C and 507°C with 31.49% mass loss which is attributed to the elimination of 4-methylphenyl group of L<sub>1</sub> ligand and two pyridine rings with methyl units. In the second step, the mass loss of 24.77% is observed between 507°C and 900°C due to the removal of the 1H-imidazo-[4,5-f]-[1,10]-phenanthroline. After this decomposition step, the residue with the mass 43.74% may be assigned to two fluoro units, two phenyl groups of 2-phenylpyridine ligands and iridium [1,29]. The thermal decompositions of compounds 2 and 3 occur at two steps. Firstly, the imidazole moiety and substituted phenyl group of corresponding ligand and two methyl units of 2-phenylpyridine ligands undergo decomposition in the temperature range 30°C and 507°C. After this decomposition step, the mass loss is around 24.00% corresponding to the elimination of the two fluoro units and phenanthroline part of corresponding ligand. The residue with 55% may be associated with two 2-phenylpyridine ligands and iridium. The thermal decomposition steps of compound 4 are shown in Table S1. Compound 4 shows lower decomposition temperature (221°C) than other compounds (1-3) in the presence of the phenyl group on L<sub>4</sub> ligand [6]. The obtained results show that the thermal decompositions of synthesized compounds are favorable for OLED applications [10].

#### 3.2. Absorption and photoluminescence studies

The absorption spectra of  $3 \times 10^{-6}$  M solution of the compounds (1-8) in chlorobenzene are shown in Fig. 2 and corresponding data are summarized in Table 1. The absorption bands of compounds (1-8) around 312 nm are assigned to the spin-allowed  $^1\pi \rightarrow \pi^*$  transitions of both 2-phenylpyridine and phenanthroline ligands. The lower energy absorption bands of the complexes at 426 nm are associated with mixing singlet and triplet metal ligand charge transfer ( $^1\text{MLCT}$  and  $^3\text{MLCT}$ ) transitions and  $^3\pi \rightarrow \pi^*$  transitions which are caused by the spin-orbit coupling of iridium metal center [10].

The photoluminescence properties of the compounds with [Cl]<sup>-</sup> counterion (1-4) were investigated in different solvents (toluene, chlorobenzene, dichloromethane) at room temperature. The compounds 1, 2 and 4 exhibit similar PL spectra which give green emission bands around 545 nm in chlorobenzene and around 551 nm in dichloromethane (Fig. 3). However, the spectrum of compound 3 exhibits red shift compared to other compounds (1, 2 and 4) due to the electron donor characteristic of the -OCH<sub>3</sub> group [30].

**Table 1**Absorption and emission data of the compounds ( $3 \times 10^{-6}$  M) in different solvents (Toluene, chlorobenzene,  $\text{CH}_2\text{Cl}_2$ ).

Complex	$\sigma_p$	Toluene $\lambda_{\text{abs}}^{\text{max}}$ (nm)	$\lambda_{\text{em}}^{\text{max}}$ (nm)	Chlorobenzene $\lambda_{\text{abs}}^{\text{max}}$ (nm)	$\lambda_{\text{abs}}^{\text{max}}$ (nm)	$\text{CH}_2\text{Cl}_2$ $\lambda_{\text{abs}}^{\text{max}}$ (nm)	$\lambda_{\text{abs}}^{\text{max}}$ (nm)	$\Phi_{PL}$
<b>1</b>	-0.17	310, 356, 422	543	312, 360, 426	545	284, 332, 414	550	0.67
<b>2</b>	-0.15	310, 362, 423	543	309, 361, 426	545	284, 334, 414	551	0.70
<b>3</b>	-0.27	313, 366, 424	541	314, 364, 426	559	292, 339, 420	559	0.21
<b>4</b>	-0.01	317, 367, 427	542, 600	314, 362, 426	547	294, 342, 419	552	0.75
<b>5</b>	-0.17	283, 343, 426	545	301, 362, 428	549	272, 331, 415	570	0.74
<b>6</b>	-0.15	285, 342, 426	545	301, 362, 428	549	272, 331, 415	571	0.77
<b>7</b>	-0.27	283, 341, 429	546	302, 367, 430	559	271, 333, 423	595	0.45
<b>8</b>	-0.01	285, 343, 428	543	307, 354, 428	546	272, 332, 421	566	0.83

 $\sigma_p$  values were obtained from [43].

In toluene, the compound 4 with phenyl substituent exhibits interesting emission behavior which gives two emission bands at 542 nm and 600 nm, although it was expected that compound 4 may show broad single band like other compounds (1, 2, 3). It was observed that the intensity ratio between the emission bands 542 nm and 600 nm increases from 0.80 to 1.11 (Fig. 4) and the excitation bands are broadened with the increasing the concentrations of solutions of compound 4 from  $3 \times 10^{-7}$  to  $3 \times 10^{-6}$  M (Fig. 5) [6]. This can be attributed to the excimer emission of the molecules which can be caused by increasing intermolecular interactions in toluene as nonpolar solvent [31,32]. In toluene, the compound 4 molecules can easily contact each other by the reduction of the interactions between the complex and solvent molecules [32]. So, the  $\pi$ - $\pi$  interactions of phenyl group in compound 4 may increase and result the formation of excimer. Among the compounds containing phenyl substituents, the compound 8 with  $[\text{PF}_6^-]$  counterion exhibits broad single band and denotes no excimer formation in contrast to the compound 4 with  $[\text{Cl}^-]$  counterion. It is known from literature [33] that the anion size of  $\text{PF}_6^-$  is larger than  $\text{Cl}^-$ . The larger size of  $\text{PF}_6^-$  may decrease intermolecular interactions in toluene which may prevent the formation of excimer. Furthermore, it was observed that the emission maxima of the compounds are slightly red-shifted with increasing polarity of solvents (toluene < chlorobenzene < dichloromethane) (Table 1) [34].

The PL quantum yields of the compounds (1-8) were calculated according to the literature [34] and fac-Ir(bpy)<sub>3</sub> was used as the reference material ( $\Phi_{PL} = 0.4$  in toluene) [35]. The PL quantum yields of the compounds with  $[\text{Cl}^-]$  counterion (1-4) were found between 0.21 and 0.75 (Table 1). The PL quantum yields of the synthesized compounds are slightly higher than the related classes of iridium complexes containing mixtures of bipyridine and phenanthroline ligands [30,36,37]. This can be related to the extension of the  $\pi$ -electron conjugation of 2-phenylimidazo[4,5-f][1,10]-phenanthroline ligands which may result an increase in PL quantum yields. The high quantum yields of the compounds are important to increase the performance OLED devices. With the aim to obtain higher quantum yield in iridium complexes, the effect of  $[\text{Cl}^-]$  and  $[\text{PF}_6^-]$  counter anions on PL quantum yield have been investigated. Increased PL quantum yield was observed in the presence of  $[\text{PF}_6^-]$  counter anion compared to the compounds with  $[\text{Cl}^-]$  counterion (Table 1). The larger size of  $[\text{PF}_6^-]$  counter anion may decrease intermolecular interactions and self-quenching which may result an increase in quantum yield of compounds [13].

### 3.3. Electrochemical data

The electrochemical measurements were performed using Ag wire reference electrode, Pt wire counter electrode, glassy carbon working electrode in acetonitrile with 0.1 M TBAPF<sub>6</sub>. The cyclic voltammograms of the compounds (1-8) are shown in Fig. 6 and the data are given in Table 2. The cyclic voltammograms of the compounds exhibit two oxidation and two reduction peaks. The

oxidation peaks at around 1.22 V and 1.50 V can be associated with the metal-centered Ir(III)/Ir(IV) oxidation couple and the phenyl fragment of 2-phenylpyridine, respectively [36,38]. The reduction peaks are observed at around -1.19 V and -1.47 V are due to the pyridine fragment of 2-phenylpyridine and phenanthroline ligands, respectively. The oxidation potentials of compounds 4 and 8 containing phenyl group on 2-phenylimidazo[4,5-f][1,10]-phenanthroline are slightly shifted to anodic area when compared to the other compounds (1-3 and 5-7). It is attributed to the delocalization of  $\pi$  electrons around the ring. When compare to the electrochemical data of the compounds containing  $[\text{Cl}^-]$  counterion (1-4), a similar trend was observed with the compounds containing  $[\text{PF}_6^-]$  counterion (5-8). This indicates that the counter anions ( $\text{Cl}^-$  and  $\text{PF}_6^-$ ) do not have a significant effect on the electrochemical properties of compounds.

The first oxidation and the first reduction potentials were used for the determination the HOMO and LUMO energy levels of the compounds using ferrocene as an internal standard (0.46 V vs.  $\text{Ag}/\text{Ag}^+$ ) [39]. The energy levels of the compounds (1-8) are in the range of 5.60 to 5.52 eV for HOMO levels and 3.16 to 3.13 eV for LUMO levels. The HOMO and LUMO energy levels of the compounds suggest that these molecules can be used as dopant in host materials, e.g. poly(N-vinyl carbazole) (PVK), 4,4'-bis(9-carbazolyl)biphenyl (CBP), N,N'-Dicarbazolyl-3,5-benzene (mCP) for OLED applications [40-42].

### 3.4. Correlation of the photophysical and electrochemical properties with Hammett substituent constants

The photophysical and electrochemical properties of the iridium complexes were correlated with the Hammett constants. The photoluminescence maxima of the compounds with  $[\text{Cl}^-]$  counterion (1-4) were plotted against the Hammett Substituent Constants ( $\sigma_p$ ) [43] in Fig. 7. The poor correlation was observed between photoluminescence maxima and the Hammett constants of the substituents with a low regression coefficient ( $R^2 = 0.3721$  in  $\text{CH}_2\text{Cl}_2$ ,  $R^2 = 0.4189$  in chlorobenzene,  $R^2 = 0.1057$  in toluene). However, if the data point of compound 3 containing methoxy substituent are not used for the account, the linear correlations can be observed for photoluminescence maxima with regression coefficients  $R^2 = 0.8421$  in  $\text{CH}_2\text{Cl}_2$ ,  $R^2 = 0.9868$  in chlorobenzene,  $R^2 = 0.9868$  in toluene (Fig. 7). This can be related to the strong interaction methoxy substituent containing unshared electron pairs with benzene ring by resonance effect. This interaction can result enhanced the dipole moment of the complex which causes deviation from the linear correlation [44]. Similar trends were observed in the correlation of photophysical properties with the Hammett constants for the compounds with  $[\text{PF}_6^-]$  counterion (5-8) (Fig. S3).

The oxidation and reduction potentials of the compounds as a function of Hammett Substituent Constants ( $\sigma_p$ ) [43] were plotted in Fig. 8. The good linear correlation between the oxidation and reduction potentials of the compounds with  $[\text{Cl}^-]$  counterion (1-4)

**Table 2**  
The electrochemical data of the compounds (1–8) in acetonitrile.

Complex	$\sigma_p$	$E_{ox1}$ (V)	$E_{ox2}$ (V)	$E_{red1}$ (V)	$E_{red2}$ (V)	HOMO (eV)	LUMO (eV)	Band gap ( $E_g$ ) (eV)
1	-0.17	1.22	1.50	-1.19	-1.47	-5.56	-3.15	2.41
2	-0.15	1.22	1.51	-1.19	-1.47	-5.56	-3.15	2.41
3	-0.27	1.20	1.50	-1.20	-1.47	-5.54	-3.14	2.40
4	-0.01	1.26	1.53	-1.18	-1.48	-5.60	-3.16	2.44
5	-0.17	1.20	1.54	-1.20	-1.46	-5.54	-3.14	2.40
6	-0.15	1.20	1.53	-1.20	-1.46	-5.54	-3.14	2.40
7	-0.27	1.18	1.54	-1.21	-1.46	-5.52	-3.13	2.39
8	-0.01	1.23	1.54	-1.19	-1.45	-5.57	-3.15	2.42

$\sigma_p$  values were obtained from [43].

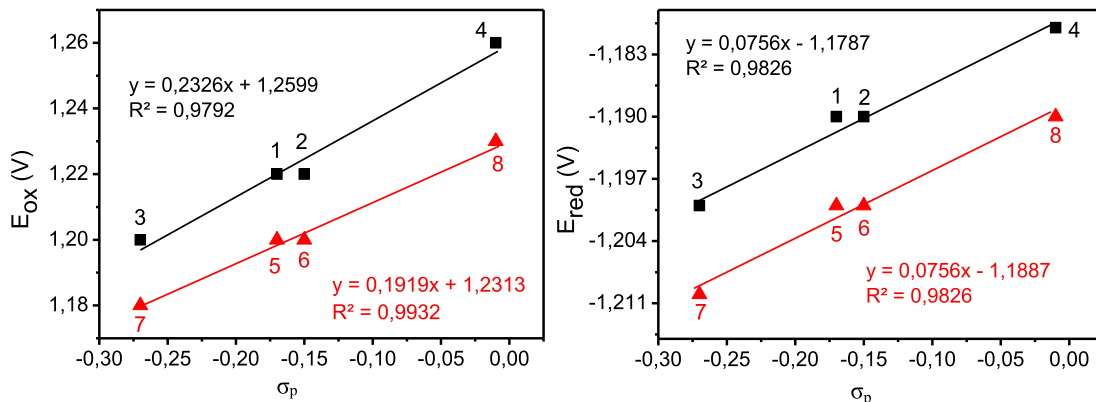


**Fig. 8.** The correlation of  $\sigma_p$  with the  $E_{ox}$  and  $E_{red}$  of the compounds (1–8).

and Hammett Substituent Constants ( $\sigma p$ ) was observed with regression coefficients  $R^2 = 0,9792$  and  $R^2 = 0,9932$  ( $R^2 = 0,9932$  and  $R^2 = 0,9826$  for the compounds with  $[PF_6^-]$  counterion (5–8)), respectively. Hammett correlations can be used to predict substituent effect on electrochemical properties of compounds.

#### 4. Conclusion

In summary, we reported the synthesis of iridium complexes containing 2-phenylimidazo[4,5-f]-[1,10]-phenanthroline with different substituents ( $-CH_3$ ,  $-CH(CH_3)_2$ ,  $-OCH_3$ ,  $-C_6H_5$ ) and the investigation of thermal, photophysical and electrochemical properties of the complexes. The synthesized complexes show thermal stability and high quantum yield in the presence of 2-phenylimidazo[4,5-f][1,10]-phenanthroline derivatives due to the extension of the  $\pi$ -electron conjugation. The effects of  $[Cl^-]$  and  $[PF_6^-]$  counter anions on PL quantum yield have been investigated. An increase in PL quantum yield of compounds was observed in the presence of  $[PF_6^-]$  counterion. The emission maxima of the compounds are red-shifted with increasing polarity of solvents and the formation of excimer is observed in the presence of phenyl substituent for compound 4 with  $[Cl^-]$  counterion in toluene. HOMO and LUMO energy levels of the compounds are calculated in the range of 5.60 to 5.52 eV and 3.16 to 3.13 eV, respectively. These results suggest that these molecules are promising candidates as dopant in OLED applications.

#### Author Contributions Section

**Cigdem Sahin:** Synthesis and characterization of molecules, Photoluminescence studies, Electrochemical and Thermogravimetric measurements, Hammett substituent constants studies, Writing- Reviewing and Editing.

**Murat Sahin:** Synthesis and characterization of molecules, Photoluminescence studies.

#### Declaration of Competing Interest

The authors declare that they have no known competing financial interests or personal relationships that could have appeared to influence the work reported in this paper.

#### Acknowledgement

We acknowledge the project support of Pamukkale University (Project No: 2014FBE057).

#### Supplementary materials

Supplementary material associated with this article can be found, in the online version, at [doi:10.1016/j.molstruc.2020.129415](https://doi.org/10.1016/j.molstruc.2020.129415).

#### References

- [1] A. Liang, J. Tang, P. Cai, X. Yang, W. Wu, L. Chen, Z. Wang, M. Cai, F. Huang, Sky-blue phosphorescent organic light-emitting diodes with dibenz-24-crown-8 substituted iridium(III) complexes as the dopant, *Dyes Pigments* 138 (2017) 77–82.
- [2] H. Yang, Y. Zhu, L. Li, Z. Zhou, S. Yang, A phosphorescent chemosensor for  $Cu^{2+}$  based on cationic iridium(III) complexes, *Inorganic Chem. Commun.* 16 (2012) 1–3.
- [3] A.C. Carrasco, V. Rodríguez-Fanjul, A. Habtemariam, A.M. Pizarro, Structurally strained half-sandwich iridium(III) complexes as highly potent anticancer agents, *J. Med. Chem.* 63 (2020) 4005–4021.
- [4] K.C. Pradhan, S. Barik, B.C. Singh, P. Mohapatra, H.K. Kisan, S. Pal, Synthesis, characterisation and theoretical studies of a series of Iridium (III) heteroleptic complexes with Schiff base ligands, *J. Mol. Struct.* 12115 (2020) 128058.
- [5] Y. Zhou, W. Li, L. Yu, Y. Liu, X. Wang, M. Zhou, Highly efficient electrochemiluminescence from iridium(III) complexes with 2-phenylquinoline ligand, *Dalton Trans.* 44 (2015) 1858–1865.
- [6] C. Sahin, A. Goren, C. Varlikli, Synthesis, characterization and photophysical properties of iridium complexes with amidinate ligands, *J. Organometallic Chem.* 772–773 (2014) 68–78.
- [7] S. Zhang, F. Wu, W. Yang, Y. Ding, Synthesis, characterization and photophysical properties of two heteroleptic 2-(4,6-difluorophenyl)pyridyl iridium(III) complexes with amidate ancillary ligands, *Inorganic Chem. Commun.* 14 (2011) 1414–1417.

- [8] E. Kabir, Y. Wu, S. Sittel, B.-L. Nguyen, T.S. Teets, Improved deep-red phosphorescence in cyclometalated iridium complexes via ancillary ligand modification, *Inorg. Chem. Front.* 7 (2020) 1362–1373.
- [9] A. Maity, K.K. Rajak, Photo induced trans→cis isomerism studies of heteroleptic iridium complex with 8-quinolinol-5-phenylazo ligand: Photophysical and electrochemical studies and its theoretical investigations, *J. Mol. Struct.* 11815 (2019) 38–47.
- [10] H. Tang, Y. Li, Q. Chen, B. Chen, Q. Qiao, W. Yang, H. Wu, Y. Cao, Efficient yellow-green light-emitting cationic iridium complexes, based on 1,10-phenanthroline derivatives containing oxadiazoletriphenylamine unit, *Dyes Pigments* 100 (2014) 79–86.
- [11] X.-H. Yang, M. Li, H. Peng, Q. Zhang, S.-X. Wu, W.-Q. Xiao, X.-L. Chen, Z.-G. Niu, G.-Y. Chen, G.-N. Li, Highly luminescent mono- and dinuclear cationic iridium(III) complexes containing phenanthroline-based ancillary ligand, *Eur. J. Inorg. Chem.* (2019) 847–855.
- [12] L. Wang, P. Cui, L. Lystrom, J. Lu, S. Kilina, W. Sun, Heteroleptic cationic iridium(III) complexes bearing phenanthroline derivatives with extended π-conjugation as potential broadband reverse saturable absorbers, *New J. Chem.* 44 (2020) 456–465.
- [13] D. Ma, L. Duan, Y. Wei, L. He, L. Wang, Y. Qiu, Increased phosphorescent quantum yields of cationic iridium(III) complexes by wisely controlling the counter anions, *Chem. Commun.* 50 (2014) 530–532.
- [14] G. Li, W. Guan, S. Du, D. Zhu, G. Shan, X. Zhu, L. Yan, Z. Su, M.R. Bryce, A.P. Monkman, Anion-specific aggregation induced phosphorescence emission (AIE) in an ionic iridium complex in aqueous media, *Chem. Commun.* 51 (2015) 16924–16927.
- [15] C. Zhong, H. Huang, A. He, H. Zhang, Synthesis and luminescent properties of novel polymeric metal complexes with bis(1,10-phenanthroline) group, *Dyes Pigments* 77 (2008) 578–583.
- [16] H.S. Lee, Y. Ha, The new iridium(III) pyridyltetrazolate complexes for blue phosphorescence, *Mol. Crystals Liquid Crystals* 504 (2009) 67–75.
- [17] Y. Liu, K. Ye, Y. Fan, W. Song, Y. Wang, Z. Hou, Amidinate-ligated iridium(III) bis(2-pyridyl)phenyl complex as an excellent phosphorescent material for electroluminescence devices, *Chem. Commun.* 25 (2009) 3699–3701.
- [18] Q.Y. Yu, J.F. Huang, Y. Shen, L.M. Xiao, J.M. Liu, D.B. Kuang, C.Y. Su, Novel phenanthroline-based ruthenium complexes for dye-sensitized solar cells: enhancement in performance through fluoro-substitution, *RSC Adv.* 3 (2013) 19311–19318.
- [19] X. Li, J. Gui, H. Yang, W. Wu, F. Li, H. Tian, C. Huang, A new carbazole-based phenanthrenyl ruthenium complex as sensitizer for a dye-sensitized solar cell, *Inorganica Chimica Acta* 361 (2008) 2835–2840.
- [20] L.F. Tan, F. Wang, H. Chao, Y.F. Zhou, C. Weng, Ruthenium(II) mixed-ligand complex containing 2-(4'-benzyloxy-phenyl)imidazo[4,5-f][1,10]phenanthroline: Synthesis, DNA-binding and photocleavage studies, *Journal of Inorganic Biochemistry* 101 (2007) 700–708.
- [21] L.F. Tan, H. Chao, Y.F. Zhou, L.N. Ji, Synthesis, characterization, DNA-binding and DNA photocleavage studies of [Ru(bpy)2(BPIP)]2+ and [Ru(phen)2(BPIP)]2+ (BPIP = 2-(4-biphenyl)imidazo[4,5-f][1,10]phenanthroline), *Polyhedron* 26 (2007) 3029–3036.
- [22] C. Dolan, R.D. Moriarty, E. Lestini, M. Devocelle, R.J. Forster, T.E. Keyes, Cell uptake and cytotoxicity of a novel cyclometalated iridium(III) complex and its octaarginine peptide conjugate, *J. Inorganic Biochem.* 119 (2013) 65–74.
- [23] Q. Zhao, S. Liu, M. Shi, F. Li, H. Jing, T. Yi, C. Huang, Tuning photophysical and electrochemical properties of cationic iridium(III) complex salts with imidazolyl substituents by proton and anions, *Organometallics* 26 (2007) 5922–5930.
- [24] C. Liu, Linpo Yu, Y. Liu, F. Li, M. Zhou, NMR study on iridium(III) complexes for identifying disulfonate substituted bathophenanthroline regio-isomers, *Magn. Reson. Chem.* 49 (2011) 816–823.
- [25] C. Jin, J. Liu, Y. Chen, G. Li, R. Guan, P. Zhang, L. Ji, H. Chao, Cyclometalated iridium(III) complexes with imidazo[4,5-f][1,10]phenanthroline derivatives for mitochondrial imaging in living cells, *Dalton Trans.* 44 (2015) 7538–7547.
- [26] F.O. Garces, Richard J. Watts, 'H and 13C NMR assignments with coordination-induced shift calculations of carbon o-bonded ortho-metallated rhodium(II) and iridium(II) complexes, *Magnetic Reson. Chem.* 31 (1993) 529–536.
- [27] H. Na, A. Maity, T.S. Teets, Bis-cyclometalated iridium complexes with electronically modified aryl isocyanide ancillary ligands, *Dalton Trans.* 46 (2017) 5008–5016.
- [28] B. Chen, Y. Li, W. Yang, W. Luo, H. Wu, Efficient sky-blue and blue-green light-emitting electrochemical cells based on cationic iridium complexes using 1,2,4-triazole-pyridine as the ancillary ligand with cyanogen group in alkyl chain, *Organic Electron.* 12 (2011) 766–773.
- [29] D. Chen, L. Han, D. Liu, K. Ye, Y. Liu, J. Zhang, Y. Wang, High performance blue-green and green phosphorescent OLEDs based on iridium complexes with N^C^N-coordinated terdentate ligands, *RSC Adv.* 5 (2015) 18328–18334.
- [30] K. Hasan, A.K. Bansal, I.D.W. Samuel, C. Roldan-Carmona, H.J. Bolink, E. Zysman-Colman, Tuning the emission of cationic iridium (iii) complexes towards the red through methoxy substitution of the cyclometalating ligand, *Scientif. Rep.* 5 (2015) 12325, doi:10.1038/srep12325.
- [31] J. Zhao, L. Liu, J. Wu, J. Yu, Spectral variation of solution-processed blue bis[(4,6-difluorophenyl)-pyridinato-N,C2'] (picolinate) iridium(III) phosphor, *Dyes Pigments* 102 (2014) 234–240.
- [32] S. Takayasu, T. Suzuki, K. Shinozaki, Intermolecular interactions and aggregation of fac-Tris(2-phenylpyridinato-C2',N)iridium(III) in nonpolar solvents, *J. Phys. Chem. B* 117 (2013) 9449–9456.
- [33] J.N. Gayton, S. Autry, R.C. Fortenberry, N.I. Hammer, J.H. Delcamp, Counter anion effect on the photophysical properties of emissive indolizine-cyanine dyes in solution and solid state, *Molecules* 23 (2018) 3051, doi:10.3390/molecules23123051.
- [34] J. Xu, C. Yang, B. Tong, Y. Zhang, L. Liang, M. Lu, The effects of different solvents and excitation wavelength on the photophysical properties of two novel Ir(III) complexes based on phenylcinnoline ligand, *J. Fluorescence* 23 (2013) 865–875.
- [35] L. Chen, Z. Ma, J. Ding, L. Wang, X. Jinga, F. Wang, Self-host heteroleptic green iridium dendrimers: achieving efficient non-doped device performance based on a simple molecular structure, *Chem. Commun.* 47 (2011) 9519–9521.
- [36] S. Salinas, M.A. Soto-Arriaza, B. Loeb, New iridium cyclometallated complexes with potential application in OLED, *Polyhedron* 30 (2011) 2863–2869.
- [37] R. Cao, J. Jia, X. Ma, M. Zhou, H. Fei, Membrane localized iridium(III) complex induces endoplasmic reticulum stress and mitochondria-mediated apoptosis in human cancer cells, *J. Med. Chem.* 56 (2013) 3636–3644.
- [38] C. Sahin, A. Goren, S. Demir, M.S. Cavus, New amide based iridium(III) complexes: synthesis, characterization, photoluminescence and DFT/TD-DFT studies, *New J. Chem.* 42 (2018) 2979–2988.
- [39] B.S. Kim, S.H. Kim, Y.S. Kim, S.H. Kim, Y.A. Son, Synthesis and characterization of quinoline-based dye sensor, *Mol. Crystals Liquid Crystals* 504 (2009) 173–180.
- [40] H. Tang, Z. Chen, L. Wei, J. Miao, G. Meng, Y. He, H. Wu, Three cationic iridium(III) complexes with 1,10-phenanthroline or compounds containing 1,10-phenanthroline unit as auxiliary ligands: Synthesis and application in polymer light-emitting diodes, *Dyes Pigments* 131 (2016) 340–348.
- [41] H. Tang, L. Wei, G. Meng, Y. Li, G. Wang, F. Yang, H. Wu, W. Yang, Y. Cao, Polymer light-emitting diodes based on cationic iridium(III) complexes with a 1,10-phenanthroline derivative containing a bipolar carbazole–oxadiazole unit as the auxiliary ligand, *Opt. Mater.* 37 (2014) 679–687.
- [42] K.S. Yook, S.O. Jeon, C.W. Joo, J.Y. Lee, High efficiency deep blue phosphorescent organic light-emitting diodes, *Organic Electron.* 10 (2009) 170–173.
- [43] C. Hansch, A. Leo, R.W. Taft, A survey of hammett substituent constants and resonance and field parameters, *Chem. Rev.* 91 (1991) 165–195.
- [44] F.H. Westheimer, The Electrostatic Effect of Substituents on the Dissociation Constants of Organic Acids. IV. Aromatic Acids, *J. Am. Chem. Soc.* 61 (1939) 1977–1980.